2001-GT-0333

LASER VELOCIMETER MEASUREMENTS OF AXIAL VELOCITY FIELD IN THE NASA SUPERSONIC FAN ROTOR

J. Lepicovsky
Dynacs Engineering, NASA GRC Group
Cleveland, OH 44135

E.P. Braunscheidel, R.J. Bruckner
NASA Glenn Research Center
Cleveland, OH 44135

D.L. Tweedt
AP Solutions
Cleveland, OH 44135

ABSTRACT

An analysis of laser Doppler velocimeter (LDV) data for the axial velocity flowfield in the rotor of the Mach *2* inlet flow supersonic throughflow fan (SSTF) is presented in this paper. The paper starts with a short description of the SSTF test package to highlight the specifics of the SSTF operation. It is followed by a detailed description of a dedicated LDV system for measurement in a supersonic throughflow fan and the experience gained. Most of the experimental data presented were acquired in a low supersonic throughflow regime (inlet Mach number of *1.4*). The results and conclusions presented are based mainly on the experimental data only. A limited amount of computational fluid dynamics (CFD) predictions were used for comparison with the experimental results. The CFD methods, however, are not discussed in this paper. As shown in this paper, a reasonably good agreement between the LDV data and the CFD predictions was found for the low supersonic throughflow regime. The design point data (inlet Mach number of *2.0*) exhibited an unexpectedly high noise in the velocity data in comparison with the data for low supersonic throughflow operating conditions. For the off-design supersonic regime (shock in rotor), substantial differences exist between the experimental and computational data.

BACKGROUND

In the late 1980s, the NASA Glenn Research Center started a program to design, build, and test a single-stage fan that would operate with supersonic air velocities sustained through the blade rows. The program was initiated as a response to a growing interest at that time in efficient, sustained supersonic cruise technology, which could be applied to high-speed transport aircrafts. After all, the only supersonic transport airplane in regular service, Concorde, had limited commercial success, primarily because of poor fuel economy. The main advantage of a supersonic throughflow fan (SSTF) for a high-speed propulsion system is that no long and heavy inlet system is needed to decelerate flow to subsonic velocities, as is the case for conventional turbomachinery. Also, higher-pressure ratio per blade row can be achieved at higher velocities. There was no experience with a supersonic throughflow fan for an inlet Mach number of *2* at the time of the program conception. Therefore, the main goal of the work was to demonstrate feasibility, gain fundamental understanding of the flow physics, and develop an experimental database.

The supersonic throughflow fan was successfully tested in the early 1990s. After extensive tests with conventional experimental techniques to determine the basic performance map, a sizeable portion of the overall test program was devoted to tests using advanced experimental techniques, particularly a laser Doppler velocimeter (LDV) and pressure sensitive paint measurement methods. The application of advanced experimental techniques to the supersonic throughflow fan program was the lead author's responsibility. Consequently, the main focus of the paper is on experience and results obtained with a laser Doppler

velocimeter in the fan rotor, and the fan design and overall operation characteristics are mentioned marginally for the sake of completeness.

NOMENCLATURE

b_T	[mm]	blade tip axial cord
h	[mm]	blade height
m	[kg.s^{-1}]	mass flow rate
Ma_{IA}	[1]	inlet axial Mach number
n_D	[min^{-1}],[rpm]	design rotational speed
n_R	[1]	relative rotational speed
N_{RB}	[1]	number of rotor blades
r_T	[mm]	blade tip radius
u_T	[m.s^{-1}]	blade tip speed
v_{IA}	[m.s^{-1}]	inlet axial velocity
v_{AM}	[m.s^{-1}]	axial velocity at midpitch
x	[mm]	axial direction
z	[mm]	radial direction
π_F	[1]	fan stage total pressure ratio
τ	[1]	relative pitch

OBJECTIVE

The main objective of the program reported in this paper was to determine the axial velocity flowfield in the rotor of the NASA supersonic throughflow fan using a dedicated laser Doppler velocimeter system.

SSTF TEST PACKAGE

Detailed discussion of the SSTF aerodynamic design, steady state aerodynamic investigation, and performance maps are given in Refs. 1 through 4. Only a short description of the SSTF test package is given here to highlight the specifics of the SSTF operation. The overall design parameters for the SSTF pertinent to the LDV measurements are as follows:

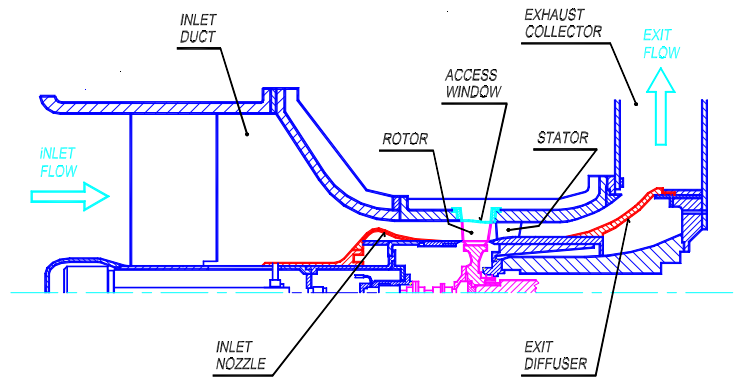|		
Blade tip speed	u_T =	457.2 m.s^{-1}
Rotational speed (design)	n_D =	17,190 min^{-1}
Mass flow rate	m =	14.29 kg.s^{-1}
Inlet axial Mach number	Ma_{IA} =	2.0
Blade tip radius (constant)	r_T =	254.0 mm
Blade height (constant)	h =	76.2 mm
Blade tip axial cord	b_T =	96.6 mm
Number of rotor blades	N_{RB} =	44

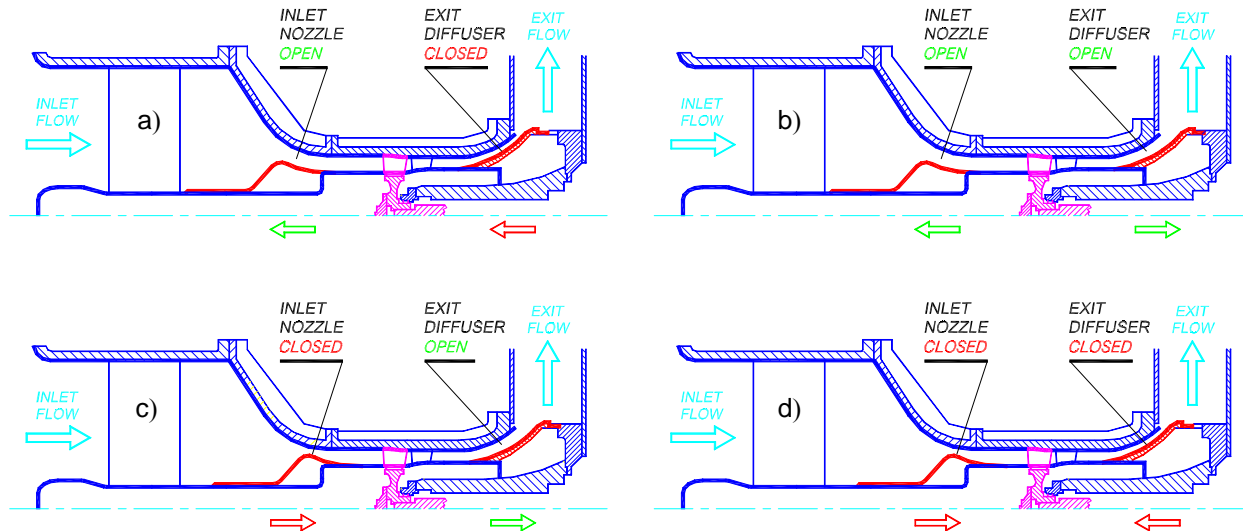**Fig. 1.   SSTF test package.**

Fig. 2.   SSTF operating regimes:
a) subsonic inflow and subsonic outlet flow,
b) subsonic inflow and supersonic outlet flow,
c) supersonic inflow and supersonic outlet flow (supersonic throughflow regime),
d) supersonic inflow and subsonic outlet flow   (shock-in-rotor regime).

2

A simplified axial section of the SSTF test package is shown in Fig. 1. The diagram shows the five main components: the SSTF rotor, stator, inlet nozzle, exit diffuser, and the laser window. Both the inlet nozzle and the exit diffuser can be translated along the fan axis to control the operating regime of the SSTF. The SSTF can operate in four distinct regimes depending on the position of the inlet nozzle and exit diffuser. The four regimes are: a) subsonic inflow and subsonic outlet flow, b) subsonic inflow and supersonic outlet flow, c) supersonic inflow and supersonic outflow (supersonic throughflow), and d) supersonic inflow and subsonic outflow (the shock-in-rotor regime). The positions of the inlet and exit controlling elements for these four regimes are shown in Fig. 2.

The stage performance map for the SSTF is shown in Fig. 3. As explained in Ref. 4, the total pressure ratio is plotted as a function of the inlet Mach number to separate the subsonic and supersonic fan regimes easily in the same map. The dotted lines in the map indicate jumps in the inlet Mach number as the shock is 'swallowed' by the rotor. Operating conditions at which the LDV system was employed are indicated on the map by double circle symbols. Most of the LDV data discussed in this paper were acquired for a low supersonic inlet velocity of Mach number *1.4* and the normalized rotational speed of $n_R = 0.75$ for either the supersonic throughflow regime (point *C*) or the off-design supersonic regime with a strong shock wave in the SSTF rotor (point *D*).

DEDICATED LDV SYSTEM

Detailed description of the LDV system layout, optical hardware, electronic hardware, traversing mechanism, and seeding apparatus is given in Ref. 5. An abbreviated description of the LDV system used follows. The photograph in Fig. 4 shows an overall view of the SSTF test facility with the LDV system on a traversing mechanism in the middle. Fig. 5 shows a view of the LDV system hardware as positioned in front of the laser window. The view of the window in the fan's shroud that allowed optical access to the rotor is in Fig. 6. As seen here, the window covered only the rotor region and did not allow access in front of the SSTF rotor or in the region of the SSTF stator.

The LDV system built for the SSTF experiment was a single-component Doppler system capable of rotating the plane of velocity measurements by ±*180 dg*. The optical layout of the LDV system is shown in Fig. 7. The LDV optical hardware consists of: (1) laser, (2) front mirrors, (3) beam waist lenses, (4) rear mirrors, (5) rotator, (6) beam splitter unit, (7) focusing lens, (8) middle mirror, (9) elliptical mirror, (10) collimating lens, (11) cradle mirrors, (12) cradle, (13) front lens, and (14) photomultiplier tube.
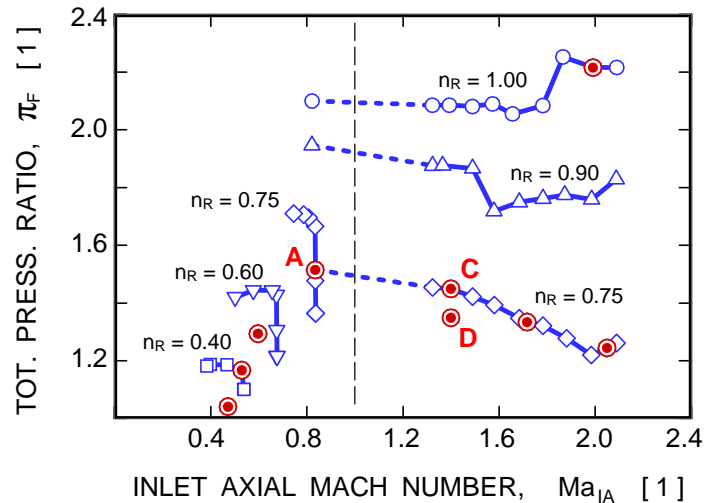
Fig. 3. LDV measurements in the SSTF performance map.
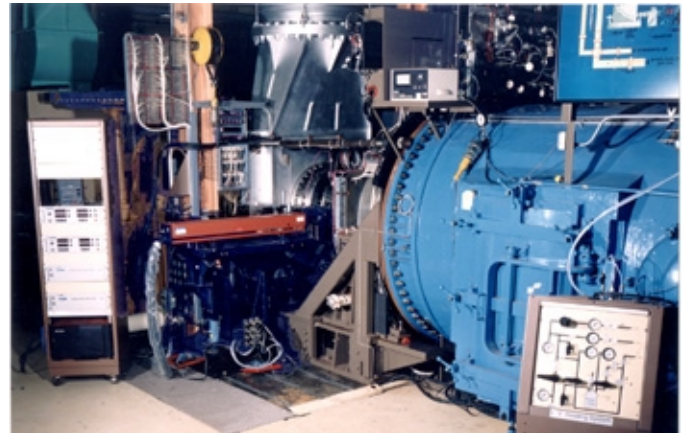
Fig. 4   Overall view of the SSTF test facility.
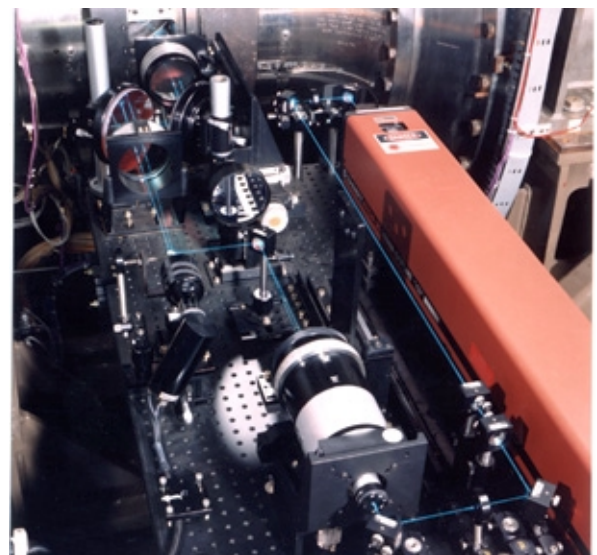
Fig. 5   LDV system positioned for measurements in the SSTF rotor.

3

A photograph of the front part of the LDV optics is in Fig. 8. The system was assembled from components designed both commercially and in-house, with a strong emphasis on ruggedness and easy adjustability. During the SSTF testing, the LDV system proved to be very stable and insensitive to the high level of vibrations and worked reliably.

Seeding is an extremely important aspect of LDV measurement in confined supersonic flows. The seeding apparatus for the SSTF tests was an atomizer-based aerosol generator which used polystyrene latex (PSL) spheres as seed particles and either water, ethyl alcohol   or a water/alcohol mixture as the carrier liquid. Three spray nozzles are shown in Fig. 9. They were located in the SSTF inlet plenum, *2 m* upstream of the LDV measurement station. The particle size diameter was *1.18 μm*.   The PSL particles were manufactured according to the procedure described in Ref. 6.

Intuitively,   monodispersed   PSL seeds are the most suitable particles for applications in confined supersonic flows. Experience, however, showed that the presence of carrier-liquid vapors in the flow constitutes a significant problem. In supersonic flows, due to the flow acceleration between the plenum and the test point conditions, the flow temperature drops below the dew point and the carrier liquid vapors condense back on the PSL spheres. The process results in liquid droplets of various diameters larger than the individual PSL spheres. The carrier liquid droplets around the PSL spheres are then the actual signal generators. As a results, even though known size PSL particles are seeded into the flow, the droplets generating the signal are larger and their actual diameter is unknown.   There are two consequences of this fact: 1) larger relaxation length after particles passed through a region with high velocity gradient, and 2) increase of apparent velocity turbulence in the same region.   An estimated   relaxation   length   for   the   shock-in-rotor condition was between *5* and *10 mm* (Ref. 7).

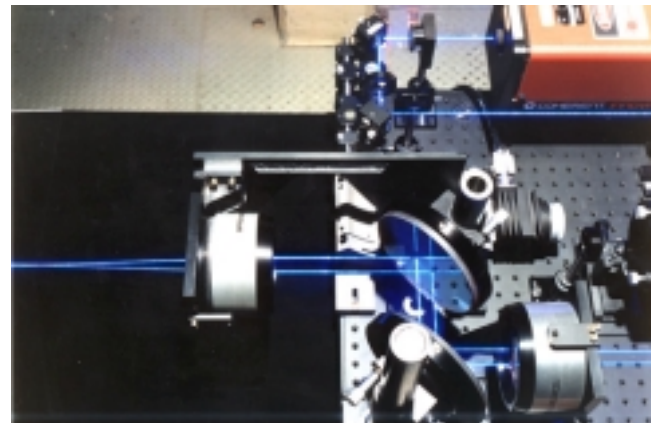**Fig. 6   SSTF rotor optical access (LDV window).**

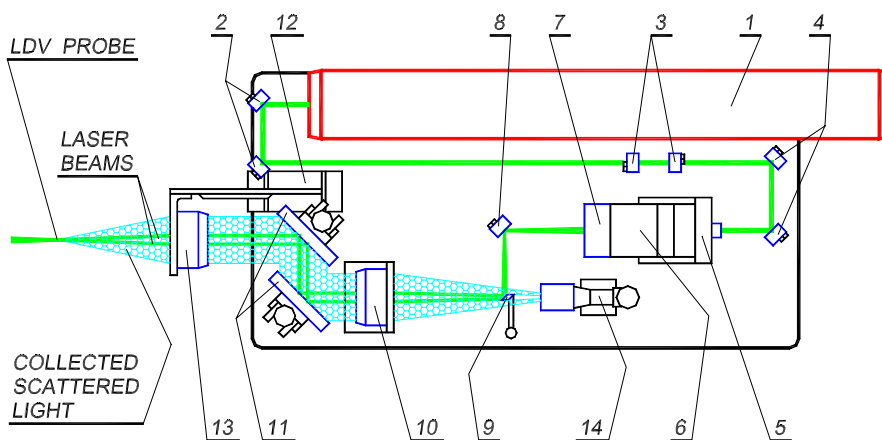**Fig. 8   Front lens of the LDV system.**

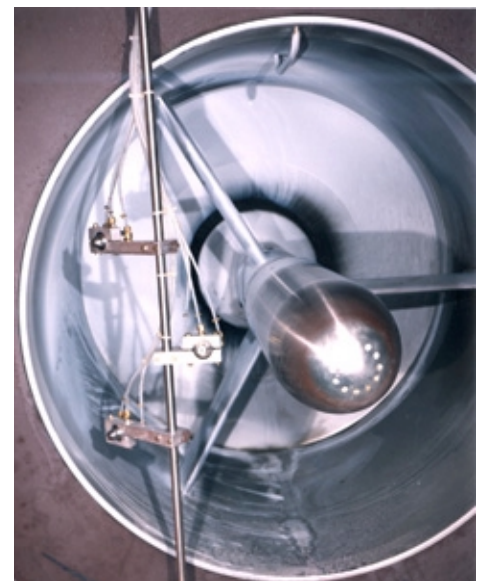**Fig. 7.   SSTF LDV system layout.**

Fig. 9   Seeding nozzles in the SSTF inlet plenum

4

EXPERIMENTAL RESULTS

All LDV data acquired during this research effort are presented in full in Ref. 5. The nature of LDV data from measurements in spinning rotors is dealt with in Ref. 8, particularly the positioning of the LDV probe with respect to moving blades and visibility restrictions due to laser beam interference with moving blades. The LDV data reduction procedure is described in full in Ref. 9

In this paper, only a limited amount of LDV data is presented for low supersonic inlet Mach number operating conditions for two regimes: a) low supersonic throughflow, and b) shock-in-rotor regimes.

Low Supersonic Throughflow Regime

Blade-to-blade average channel profiles of the axial velocity component acquired for the axial traverse for the supersonic throughflow regime of $Ma_{IA} = 1.4$ and $n_R = 0.75$ are presented in Fig. 10. The LDV data were generated as an ensemble average from all the rotor blade passages (the ensemble size was about *1000* samples). The data in Fig. 10 is shown for four axial stations. The corresponding CFD results are superimposed on the LDV data, so both results can be compared directly. The CFD data were calculated using the three-dimensional NASA code RVC3D. Details of this CFD code can be found in Refs. 10 through 12. It should be mentioned that the CFD predictions were calculated before the LDV data were acquired. The vertical bars depict the range of axial velocities in individual rotor blade channels. The arrow labeled v_{IA} in the plots indicates the flow inlet average velocity determined from pressure measurements.

Velocity distributions of the axial velocity component for both LDV and CFD data along the midline of a rotor blade channel are shown in Fig. 11. The CFD prediction indicates an initial drop of the axial velocity due to an oblique shock wave attached to the blade leading edge. Within the range of the LDV measurements, the experimental data exhibit a trend similar to the CFD prediction. It can be noticed, however, that the LDV data appears to be 'shifted' in the flow direction relative to the CFD data by approximately *5%* of the blade axial cord. Very probably, a substantial portion of the shift is due to the acceleration lag of the seed particles with respect to the changes in the flow velocity (the relaxation length for this flow condition was estimated to be at least *5 mm*).
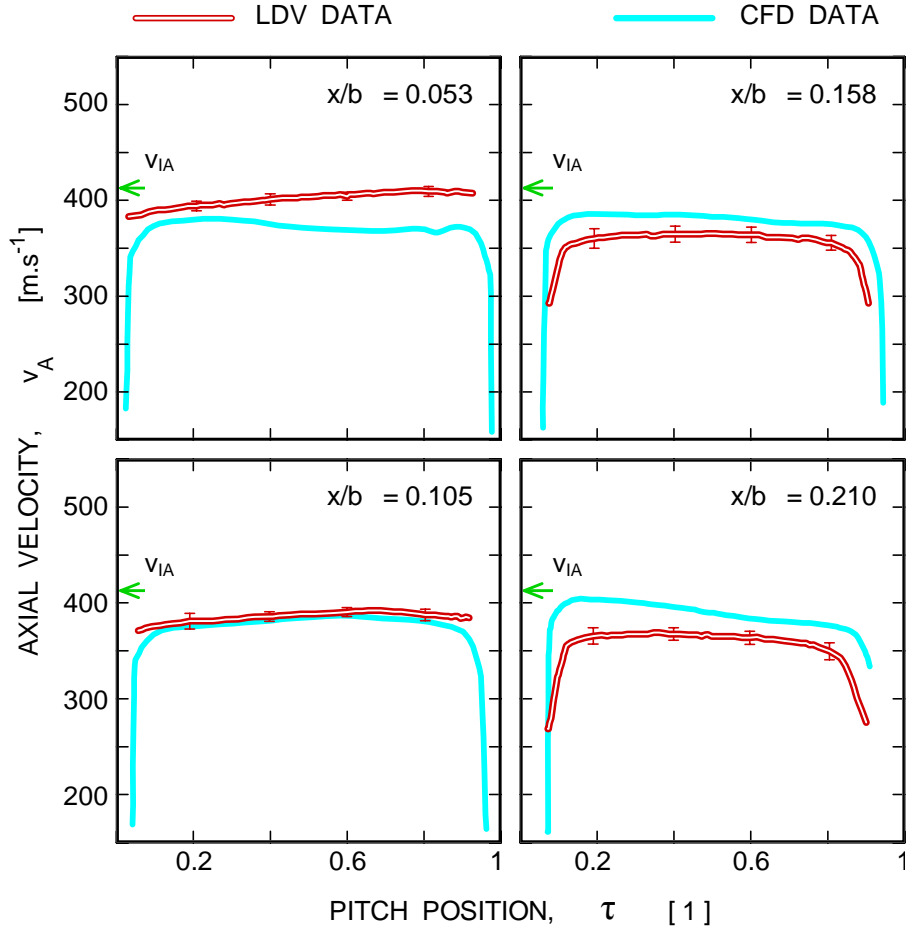

Fig. 10. Comparison of blade-to-blade LDV and CFD velocity profiles at *z/h = 0.79* for the supersonic throughflow regime of *$Ma_{IA} = 1.4$* and *$n_R = 0.75$*.
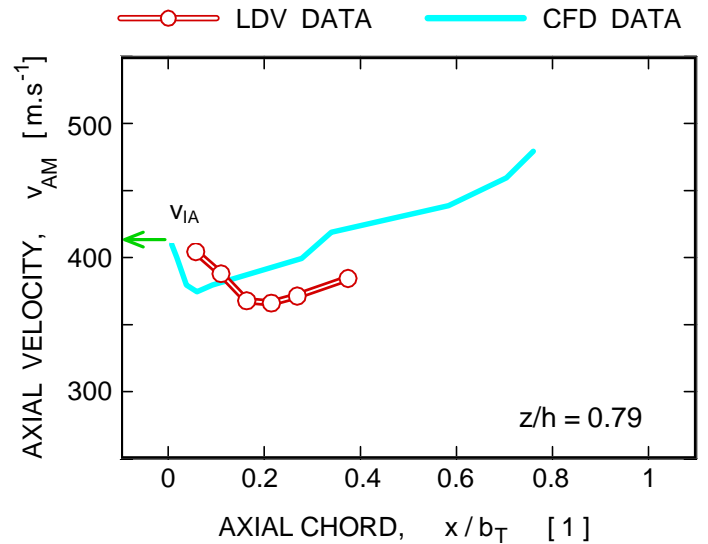

Fig. 11. Variation of midspan axial velocity along the rotor-blade passage at *z/h = 0.79* for supersonic throughflow regime of *$Ma_{IA} = 1.4$* and *$n_R = 0.75$*.

Shock-in-Rotor Regime

A shock-in-rotor off-design, supersonic regime can be induced if the SSTF operates with a supersonic inlet velocity but the exit diffuser stays partially closed, choking the outlet flow to subsonic levels. In such a case, the SSTF operates with a strong normal shock wave in the rotor.

Blade-to-blade channel-averaged axial velocity profiles are shown in Fig. 12. Fig. 13 depicts axial velocity distributions along the rotor channel midline for the LDV data. The data sets exhibit velocity deceleration which indicates the position of a strong shock wave in the rotor. There were substantial discrepancies between the CFD predictions and the LDV data and consequently the CFD predictions are not shown here. It should be stressed here that the CFD predictions for this case were made using a quasi-3D code which solves a 2D form of the Navier-Stokes equations formulated along axisymmetric stream surfaces (Ref. 10). Based on the CFD/LDV comparison, it appears that the quasi-3D code was not adequate for this application which involves substantial three dimensional flow effects.

Rotor Ensemble Averages

Rotor-average distributions, presented in Figs. 14 ($x/b_T = 0.79$) and 15 ($x/b_T = 0.32$), show velocity and velocity unsteadiness variations as ensemble averages over the rotor circumference (44 rotor blade channels). Each distribution is shown in two parts; the upper trace shows the first 22 blade channels, the lower trace shows blade channels 23 to 44. The averaging were made over 5000 rotor revolutions or more. Each ensemble set consists at least of 25 samples.

For most of the test conditions, the velocity distributions of the flowfield in the rotor appear to be quite uniform (Fig. 14). The runs exhibiting a high nonuniformity in the velocity distributions were for the unstart regime. However, the most intense nonuniformity was observed for subsonic inlet conditions at 75% of the design rotational speed (point A in Fig. 3) as shown in Fig. 15. In all cases, the nonuniformity pattern was consistent; the same blade channels were always either 'high' or 'low' regardless of the SSTF operation conditions. The repeatability of the nonuniformity pattern indicates that the velocity nonuniformity is most likely connected to the differences in the geometry of individual blade channels.
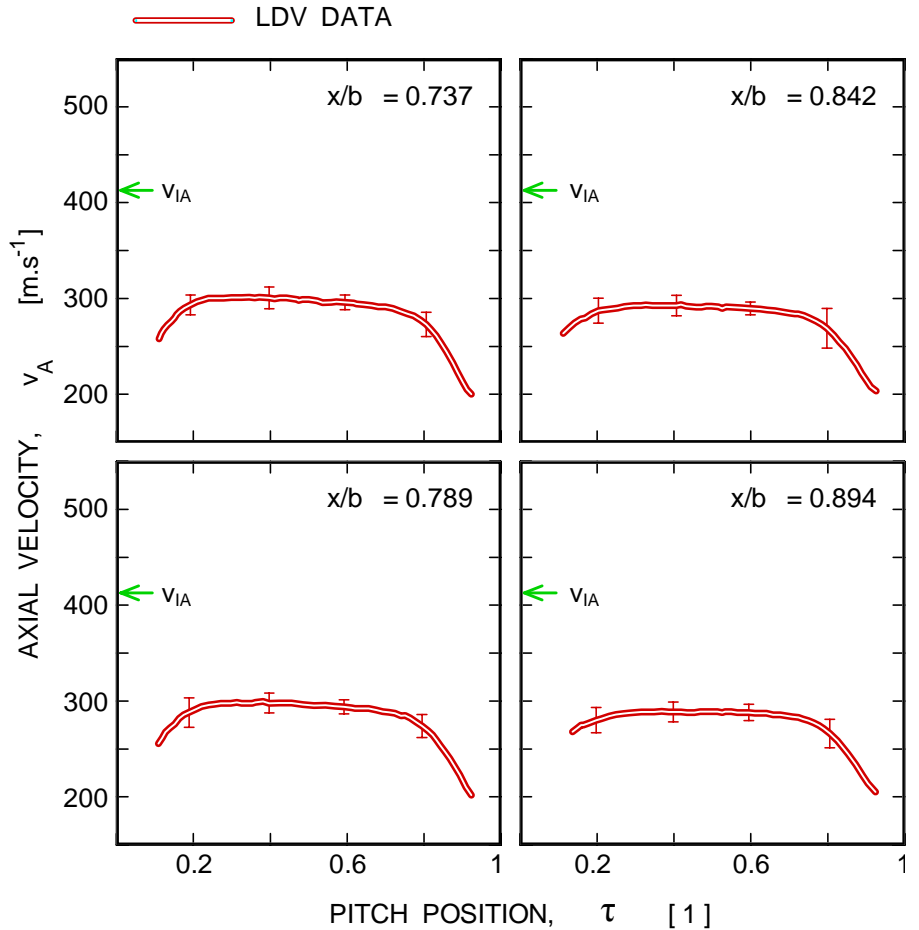

Fig. 12. Blade-to-blade LDV axial velocity profiles at *z/h = 0.79* for the supersonic shock-in-rotor regime of *Ma$_{IA}$ = 1.4* and *n$_R$ = 0.75.*
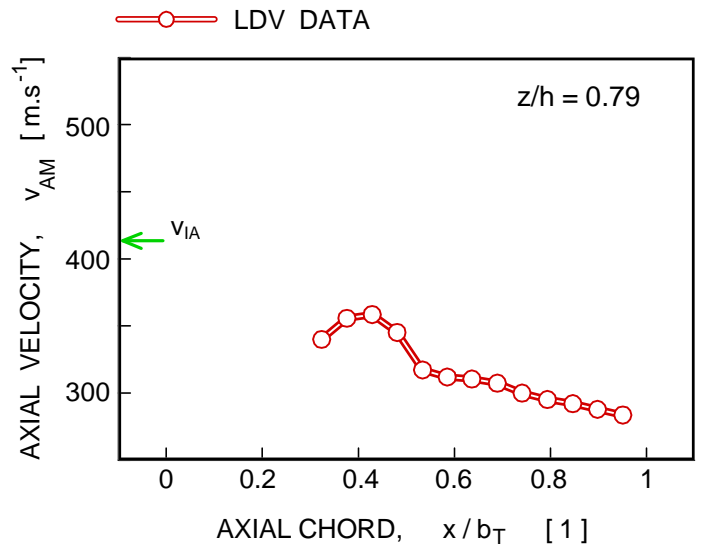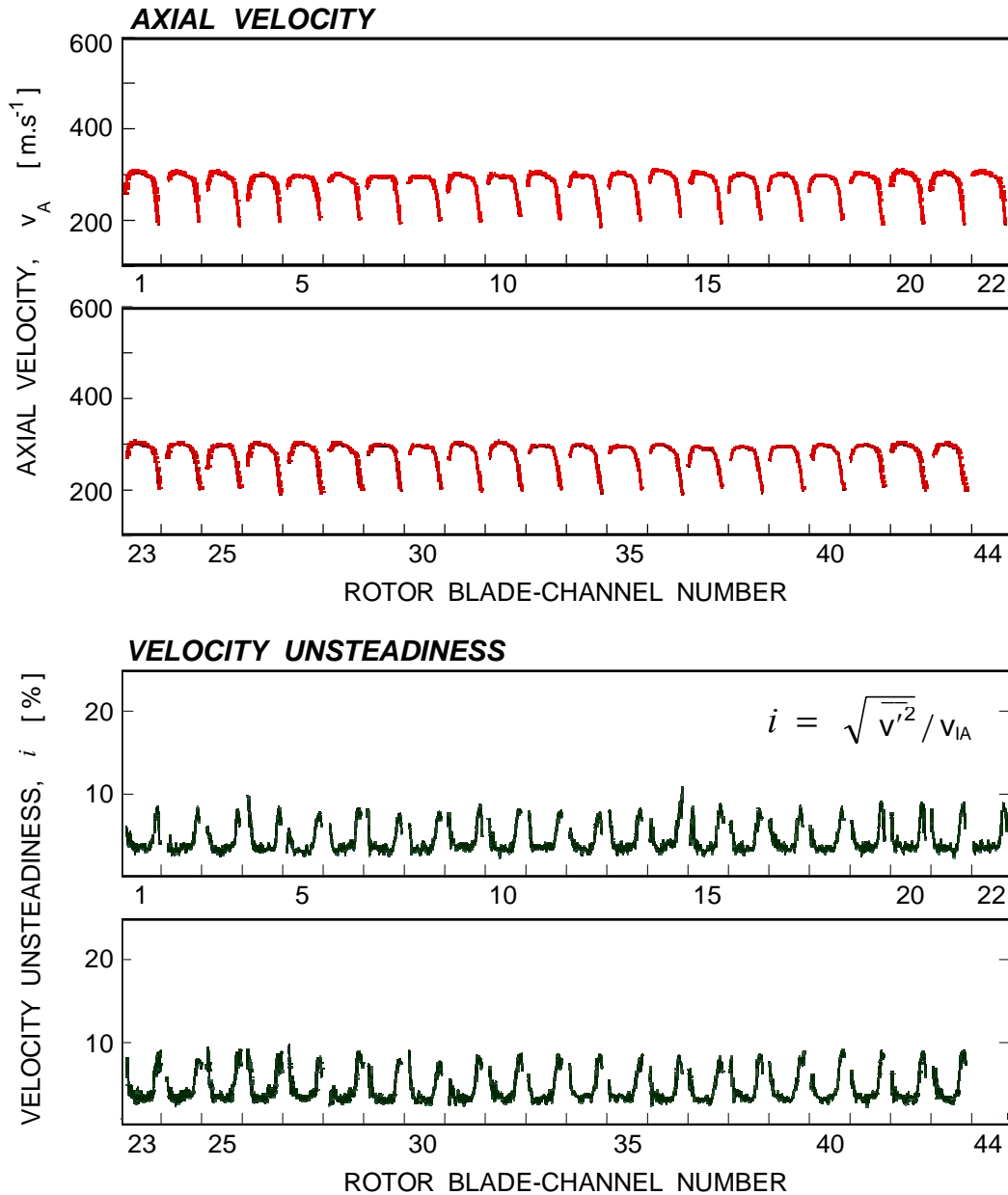

Fig. 13. Variation of midspan axial velocity along the rotor-blade passage at *z/h = 0.79* for the supersonic shock-in-rotor regime of *Ma$_{IA}$ = 1.4* and *n$_R$ = 0.75.*

AXIAL VELOCITY

VELOCITY UNSTEADINESS

$$i = \sqrt{\overline{v'^2}}\,/\,v_{IA}$$

**Fig. 14   Rotor ensemble-averaged distributions at $x/b_T = 0.79$ and $z/h = 0.79$
for supersonic throughflow regime of $Ma_{IA} = 1.4$ and $n_R = 0.75$.**

Two-Dimensional Velocity Fields

The LDV data acquired for axial and radial traverses were reduced into a form of two dimensional plots in order to facilitate easy comparison with available CFD predictions. Fig. 16 shows data for the low supersonic throughflow regime of $Ma_{IA} = 1.4$. The upper channel depicts the LDV data, while the lower channel shows the CFD prediction. The character of both flowfields is similar, however the LDV data field seems to be 'shifted downstream' by about *5%* of the blade chord. As mentioned above, the shift is probably caused by the lag of seed particles. This shift can be also traced in the radial survey plots . The data shown in the upper half of

Fig. 17 are for the axial station at about *16%* chord; the LDV data is in the left-hand channel and the CFD prediction is in the right-hand channel. There are noticeable differences in these flow patterns. The data agreement visibly improves if LDV data from the axial station at *11%* chord is compared to the CFD prediction for the axial station at *16%* chord, which is shown in the lower half of Fig. 17. It appears that due to the seed particle lag the LDV data at a given axial station actually depicts the flow pattern some distance upstream of the measurement station. It appears as if the particles 'remembered' the previous flow condition. This 'memory distance' is determined by the particle relaxation length.

7

AXIAL VELOCITY

VELOCITY UNSTEADINESS

$$i = \sqrt{\overline{v'^2}} / v_{IA}$$
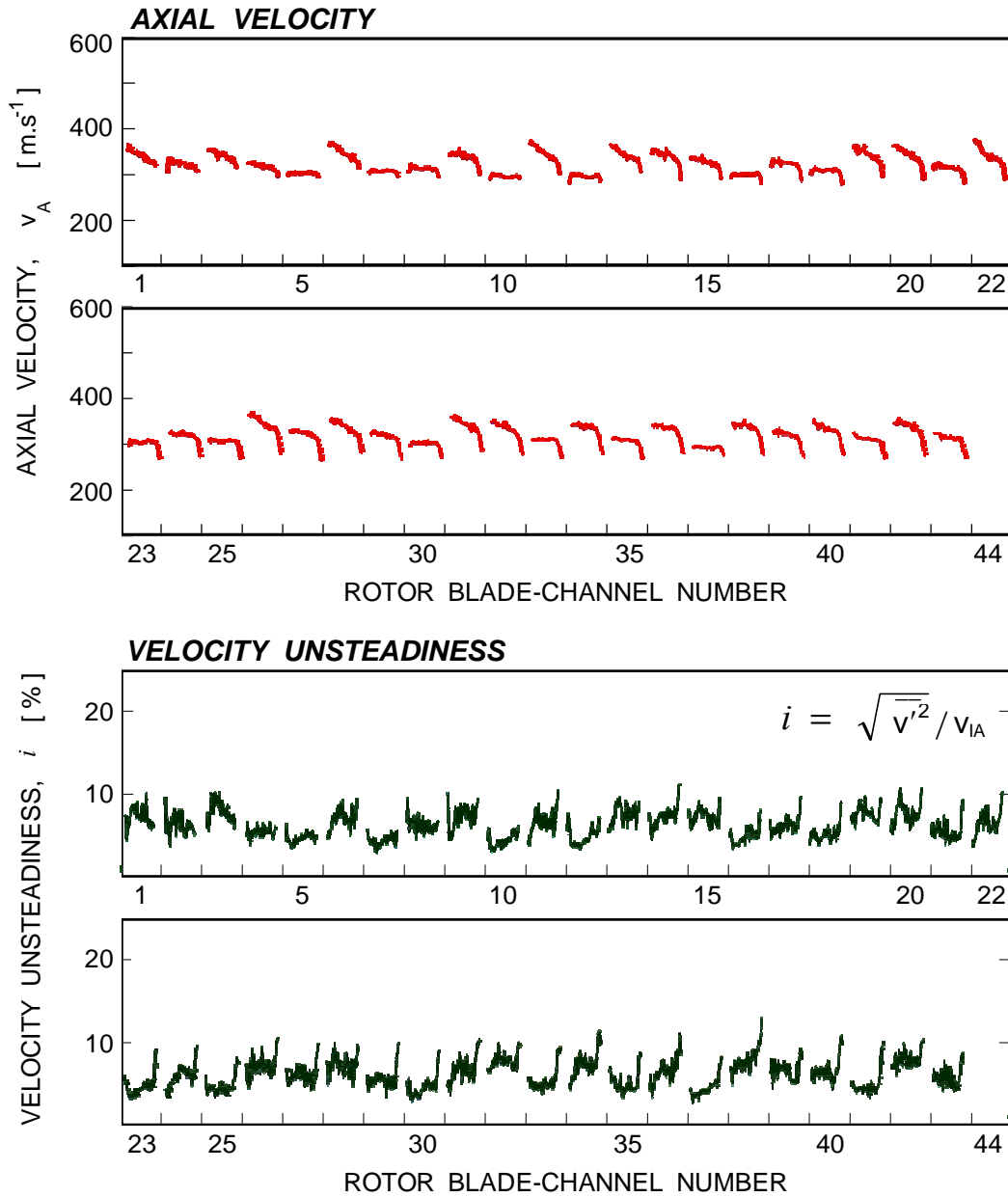
Fig. 15 **Rotor ensemble-averaged distributions at $x/b_T = 0.316$ and $z/h = 0.67$ for subsonic inlet flow regime of $Ma_{IA} = 0.83$ and $n_R = 0.75$.**

Ensemble averaged LDV data also contains information about velocity unsteadiness. Fig. 18 depicts velocity and unsteadiness for the axial station at *16%* chord. The velocity field is in the left channel, the unsteadiness field in the right channel. The velocity unsteadiness is normalized by the average inlet axial velocity. The unsteadiness exhibits a very distinct peak at about *25%* blade height. The abrupt increase in the unsteadiness level can be observed better in Fig. 19, where the same data is plotted in a three-dimensional form. The high levels of unsteadiness at the blade surfaces can be an artifact of blade surface 'jitter' during ensemble averaging or due to a poor signal-to-noise

ratio in the LDV data caused by laser-beam / blade-surface interaction. However, the high peak of unsteadiness in the middle of the blade channel at *25%* blade height seems to be genuine flow unsteadiness. A reason for the unsteadiness local maximum in the lower half of the blade is not readily obvious.

Finally, the last figure, Fig. 20, shows the velocity field that resulted from the axial survey performed at the off-design supersonic operation with a normal shock in the rotor. The data should be viewed in conjunction with data presented in Fig. 13 that shows velocity distribution along the midpitch line.

Velocity field units: [m.s⁻¹]
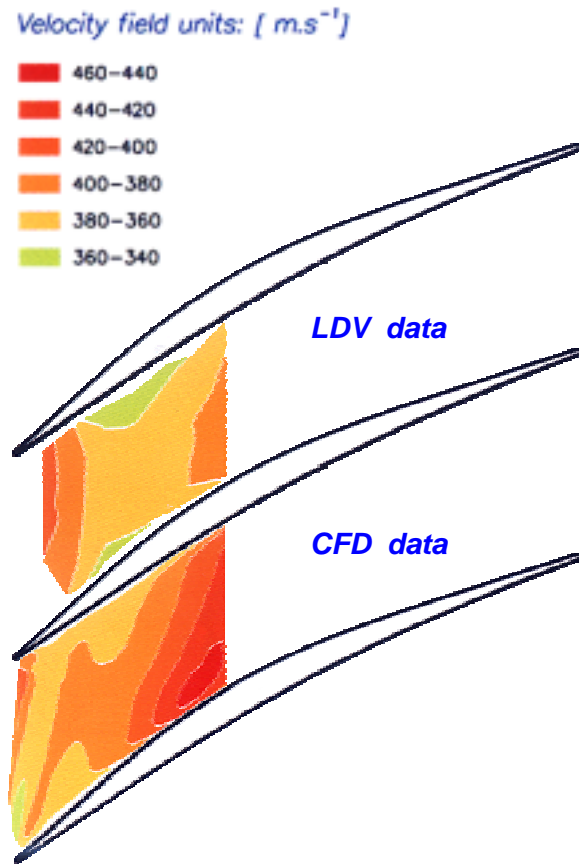
Fig. 16   **Comparison of LDV experimental data and CFD prediction for axial survey for low supersonic through flow regime (Ma_{IA} = 1.4, n_R = 0.75, z/h = 0.79).**

CONCLUSIONS

The conclusions reached during the course of this work can be divided into two categories. The first one includes comparisons between the LDV data and the CFD predictions as well as the aerodynamics of the SSTF rotor. The second category deals with lessons learned about the applied experimental technique.

In general, the LDV results corrected for the seed particle lag agreed reasonably well with the CFD predictions for low supersonic throughflow (Ma_{IA} = 1.4; n_R = 0.75) and design-point throughflow (Ma_{IA} = 2.0; n_R = 1.0) operating regimes (the design-point throughflow data were not presented in this paper). For the off-design, shock-in-rotor supersonic regime, however, noticeable differences were found between the LDV and CFD results. The LDV data indicated significant channel-to-channel velocity variations for some of the off-design regimes investigated. The recorded velocity unsteadiness is potentially useful information, which may help to identify at least some sources of loss in the flow.
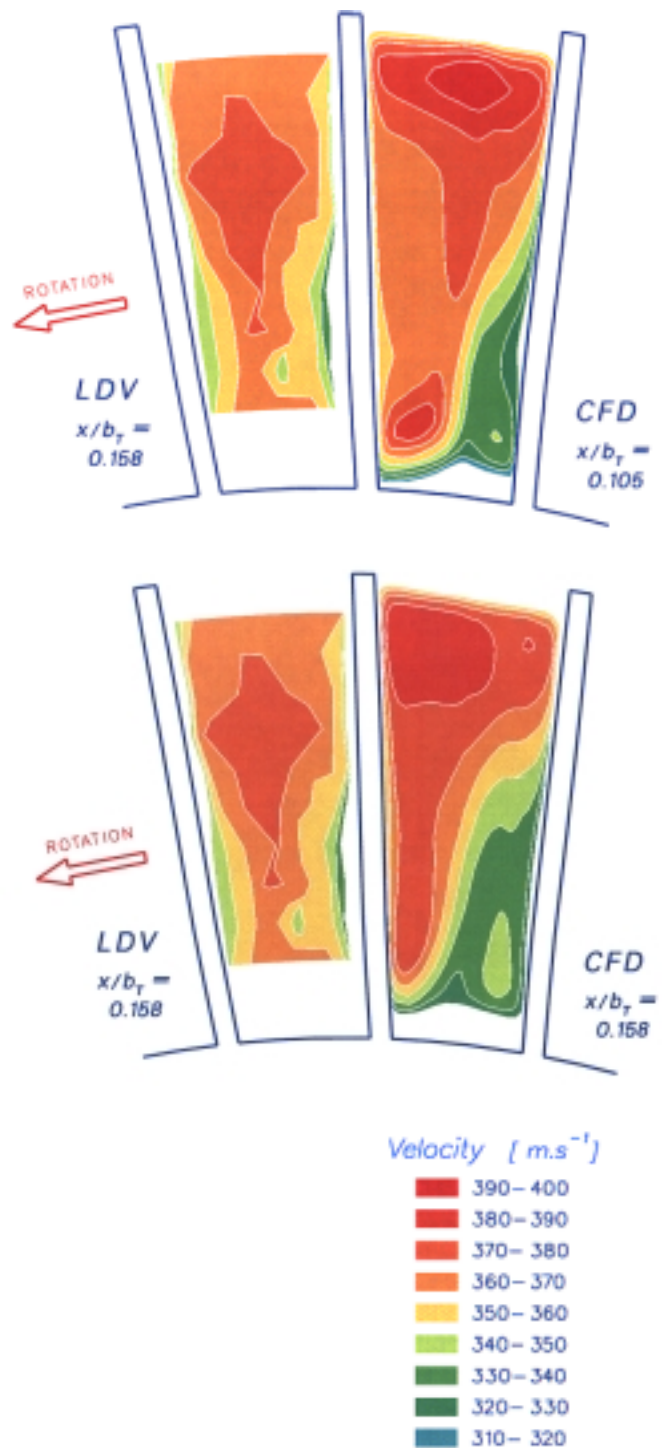
Fig. 17   **Comparison of radial surveys of LDV data at x/b_T = 0.158 and CFD predictions at two axial stations of x/b_T = 0.105 and 0.158 for low supersonic throughflow regime (Ma_{IA} = 1.4; n_R = 0.75).**

The experimental results demonstrate that laser velocimetry is a viable experimental technique for this type of application. The results proved to be repeatable, exhibited expected trends, and revealed new information. The measured velocities in the rotor correlated very well with velocities at the rotor inlet as determined from independent pressure measurements. The accuracy of the LDV measurements is estimated to be better than $\pm 7\%$ of the actual flow velocity. The major source of uncertainties in the LDV data, stems from the lag effects of seed particles, particularly in supersonic flows with complex shock structures. In particular, the selected method of seeding, spraying a volatile carrier liquid that contained solid particles, very reliable and widely used in subsonic flows, seems not to be adequate in supersonic flows due to the subsequent vapor condensation as the flow accelerates and the flow temperature drops. Attention to this problem will be necessary for further improvements in the accuracy of LDV measurements in the SSTF environment.
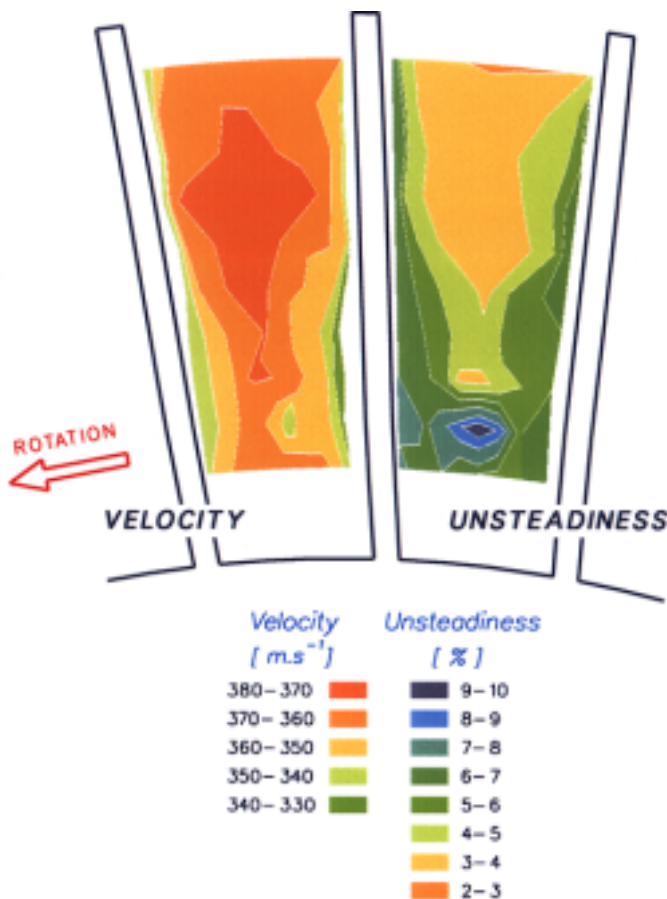
Fig. 18   Measured velocity and unsteadiness fields for a radial survey at *16%* chord for low supersonic throughflow regime ($Ma_{IA} = 1.4$, $n_R = 0.75$, $x/b_T = 0.158$).

REFERENCES
1. Schmidt, J.F., Moore, R.D., Wood, J.R., and Steinke, R.J.: "Supersonic Throughflow Fan Design", NASA TM-88908, 1987.
2. Urasek, D.C., Cunnan, W.S., Lantz, R.L., Fronek, D.L., Dawson, R.A., and Brown, J.C.: "Supersonic Throughflow Fan Test Facility at NASA Lewis Research Center", NASA TP-3038, 1990.
3. Tweedt, D.L.: "The Aerodynamics of a Baseline Supersonic Throughflow Fan Rotor", NASA TM-106651, 1994.
4. Moore, R.D., Braunscheidel, E.P., and Tweedt, D.L.: "Aerodynamic Performance of a Supersonic Throughflow Fan Stage with a Convergent Flow Path", NASA TP-3530, 1995.
5. Lepicovsky, J.: "A Collection of Laser Velocimeter Data from a Supersonic Throughflow Fan Rotor", NASA CR-195391, 1994.
6. Nichols, C.E., Jr.: "Preparation of Polystyrene Microspheres for Laser Velocimetry in Wind Tunnels", NASA TM 8913, 1987.
7. Lepicovsky, J. and Bruckner, R.J.: "Seeding for Laser Velocimetry in Confined Supersonic Flows with Shocks", NASA TM 107265, 1996.
8. Lepicovsky, J.: "Coupling of Laser Velocimeter Data with Geometry of the Supersonic Throughflow Fan Rotor", NASA CR-194459, 1993.
9. Lepicovsky, J.: "Data Reduction Procedures for Laser Velocimeter Measurements in Turbomachinery Rotors", NASA CR 195343.
10. Chima, R.V.: "Explicit Multigrid Algorithm for Quasi-Three-Dimensional Viscous Flows in Turbomachinery," *Journal of Propulsion and Power*, Vol. 3, pp. 397-405, 1987.
11. Chima, R.V. and Yokota, J.W.: "Numerical Analysis of Three-Dimensional Viscous Internal Flows," *AIAA Journal*, Vol. 28, pp. 798-806, 1990.
12. Chima, R.V.: "Viscous Three-Dimensional Calculations of Transonic Fan Performance," NASA TM-103800, 1991.
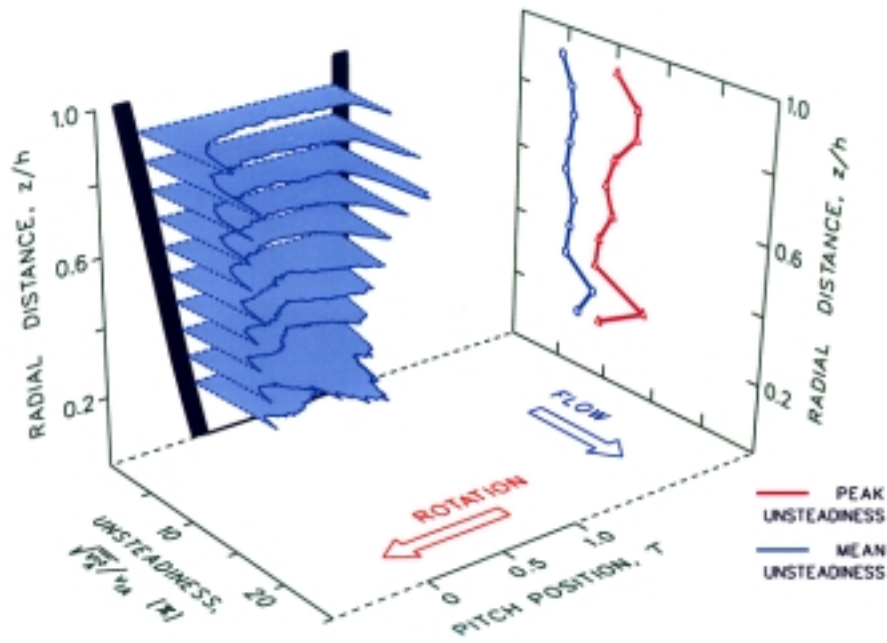
Fig. 19 Measured velocity unsteadiness field for a radial survey at *16%* blade chord for low supersonic throughflow regime of $Ma_{IA} = 1.4$ and $n_R = 0.75$ $(x/b_T = 0.158)$.
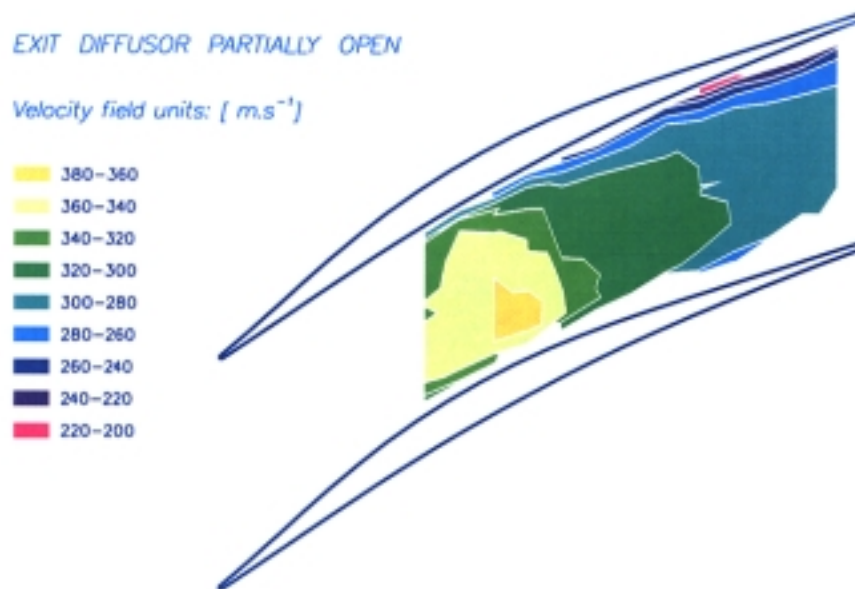

EXIT DIFFUSOR PARTIALLY OPEN

Velocity field units: [m.s^{-1}]

- 380–360
- 360–340
- 340–320
- 320–300
- 300–280
- 280–260
- 260–240
- 240–220
- 220–200

Fig. 20 Measured velocity field for axial survey for low supersonic off-design flow regime with normal shock in rotor $(Ma_{IA} = 1.4; n_R = 0.75, z/h = 0.79)$.

11